

## Use of ionic liquids based on phosphonium salts for preparing biocomposites by *in situ* polymerization

Grazia Totaro, Paola Marchese, Laura Sisti, Annamaria Celli

Dipartimento di Ingegneria Civile, Chimica, Ambientale e dei Materiali, Università di Bologna,

Via Terracini 28, 40131 Bologna, Italy

Correspondence to: G. Totaro (E-mail: grazia.totaro@unibo.it)

**ABSTRACT:** A sodium montmorillonite, Dellite HPS, was modified with ionic liquids based on phosphonium salts, such as octadecyltriphenylphosphonium tetrafluoroborate and octadecyltriphenylphosphonium bromide. Thanks to their high thermal stability, these salts can be used during *in situ* polymerization, a method that favors the achievement of a good dispersion of the clay. Poly(1,4-dimethylcyclohexane adipate) (PCHA), was chosen as an example of aliphatic polyester which can be a suitable matrix for new biocomposites with organo-clays. The organo modified clays prepared were characterized by X-ray diffraction (XRD), ATR-FTIR spectroscopy, and thermal gravimetric analysis (TGA) while biocomposites were analyzed in terms of molecular structure, thermal and thermomechanical properties. The degree of dispersion of the clays in the polymer matrix was studied by XRD. The results show that the clays are well dispersed in the biocomposites, despite an intercalated structure highlighted by XRD analysis. Moreover, the clays confer a certain improvement in mechanical properties to the final materials. © 2015 Wiley Periodicals, Inc. *J. Appl. Polym. Sci.* **2015**, *132*, 42467.

**KEYWORDS:** biomaterials; ionic liquids; thermal properties

Received 23 December 2014; accepted 7 May 2015

DOI: 10.1002/app.42467

### INTRODUCTION

Today, composites represent an opportunity to prepare high-performance materials for advanced applications. Some of the most promising nanoscaled fillers are layered silicate nanoclays such as montmorillonite (MMT), which belongs to the structural family known as the 2 : 1 phyllosilicates. Its crystal structure consists of layers made up of two silica tetrahedral sheets fused to an edge-shared octahedral sheet of either aluminium or magnesium hydroxide. Stacking of the layers leads to a regular van der Waals gap between the layers (the interlayer or gallery). Isomorphic substitution within the layers generates charge deficiency (i.e.  $\text{Fe}^{2+}$  or  $\text{Mg}^{2+}$  replacing  $\text{Al}^{3+}$  in MMT). The deficit charges are compensated by cations (usually  $\text{Na}^+$  or  $\text{K}^+$ ) absorbed between the three-layer clay mineral sandwiches. These are held relatively loosely and give rise to the significant cation-exchange properties.<sup>1</sup>

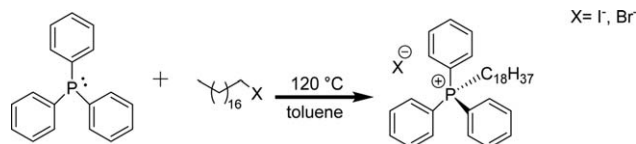
The efficiency of the MMT in improving the properties of the polymeric materials is strongly determined by the degree of its dispersion in the polymer matrix. However, the hydrophilic nature of the MMT surface often hinders a homogenous dispersion of the nanofiller in the hydrophobic polymeric matrix. Some strategies can be applied to overcome this problem. Firstly, the MMT surface can be modified by ion-exchange reactions, involving the exchange between organic cationic

surfactants with the interlayer cations. The role of the organic cation is to reduce the surface energy of the MMT surface, improving the wetting characteristics with the organic polymer.<sup>2</sup> The process leads to an increment in thickness of the interlayer gallery, which in turn favors the formation of intercalated and exfoliated nanocomposites. On the other hand, the method of preparation of nanocomposites can influence the efficacy in MMT dispersion. It has been demonstrated that the *in situ* polymerization makes it possible to obtain composites with a good degree of dispersion.<sup>3</sup>

Therefore, the combination of two approaches, modification of nanoclays and *in situ* polymerization, can be a winning strategy to prepare new composites and will be applied in this work.

Commonly organic modifiers for MMT are ammonium compounds, which suffer a poor thermal stability. Indeed, thermal stability is one of the most important properties for composite preparation and processing. Therefore, to overcome this limit, imidazolium and phosphonium compounds can be introduced as organic modifiers.<sup>1</sup>

In this study a sodium MMT, Dellite HPS, was modified with an ionic liquid based on phosphonium salts: octadecyltriphenylphosphonium bromide and octadecyltriphenylphosphonium tetrafluoroborate (Schemes 1 and 2).



**Scheme 1.** Synthesis of octadecyltriphenylphosphonium iodide and bromide.

The choice was justified on the basis of different factors: (a) ionic liquids present high thermal stability, which can be enhanced by the use of fluorinated anions;<sup>2</sup> (b) the long alkyl chains can further cooperate in the spacing of the layered silicate lamellae, while the aromatic group fits well into the hexagonal cavities of the clay; and (c) the use of phosphonium salts could enhance the heat resistance and the flame retardant properties of polymer nanocomposites.<sup>4</sup> Indeed, phosphonium salts are widely used as stabilizers in many applications: mono- and bisphosphonium salts are used as flame retardants for textiles and paper, stabilization agents for polyacrylonitrile fibers exposed to sunlight, heat stabilizers for nylon, and condensation additives to organic dyes to produce wash-fast colors.

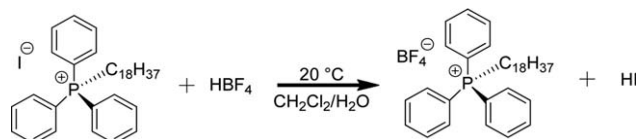
A new polymeric matrix was chosen for this study: the poly(1,4-dimethylcyclohexane adipate), an aliphatic polyester prepared from dimethyl adipate and 1,4-cyclohexanedimethanol (CHDM), potentially biobased and biodegradable.<sup>5,6</sup> Indeed, although such monomers are now petro-derived, the processes to prepare them from biomass are available.<sup>7</sup> The polymer, whose structure is reported in Figure 1, might prove interesting for future applications also because it contains the 1,4-cyclohexylene unit, that is rigid enough to notably improve thermal stability and thermal properties. Moreover, the different cis/trans ratios of the ring along the macromolecular chains endow the polymers with a wide range of properties, varying from amorphous to semi-crystalline polyesters, whose melting temperature increases with an increase in the trans content.<sup>8–11</sup>

Therefore, in the present study, some composites based on PCHA and organo-modified MMT have been prepared by *in situ* polymerization, exploiting the high thermal stability of phosphonium salts. The materials were characterized by X-ray diffraction measurements (XRD) and <sup>1</sup>H NMR. Thermal properties were investigated by thermogravimetric analysis (TGA) and differential scanning calorimetry (DSC), while mechanical performances were investigated by dynamic mechanical measurements (DMTA).

## EXPERIMENTAL

### Materials

Dellite HPS (sodium montmorillonite, MMT-Na<sup>+</sup>), with a cation exchange capacity of 128 mmol/100 g and Dellite 43B (ammonium montmorillonite containing dimethyl benzyl



**Scheme 2.** Synthesis of octadecyltriphenylphosphonium tetrafluoroborate.

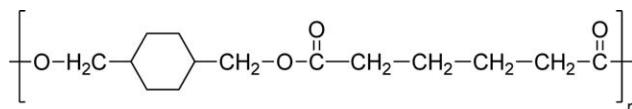


**Figure 1.** Molecular structure of poly(1,4-dimethylcyclohexane adipate) (PCHA).

hydrogenated tallow ammonium ion, MMT-NR<sub>4</sub><sup>+</sup>, cation exchange capacity of 108 mmol/100 g) were provided by Laviosa. 1,4-cyclohexanedimethanol (CHDM<sub>66</sub>) with 66 mol % of trans isomer content, dimethyl adipate (DMA), titanium tetrabutoxide (TBT), triphenylphosphine, 1-iodooctadecane, octadecyl bromide, fluoroboric acid 48 wt % in water, magnesium sulphate, toluene, hexane, ethanol, dichloromethane, and acetone, all supplied by Sigma Aldrich, were used as received without further purification.

### Methods

**Poly(1,4-dimethylcyclohexane adipate) (PCHA) Synthesis.** The homopolymer sample was prepared following the literature,<sup>5</sup> by a two-stage process, from dimethyl adipate and 1,4-cyclohexanedimethanol with 66 mol % of trans isomer content.

Dimethyl adipate (25.0 g,  $1.44 \times 10^{-1}$  mol, 1 eq), CHDM<sub>66</sub> (24.8 g,  $1.72 \times 10^{-1}$  mol, 1.2 eq), and TBT ( $5.40 \times 10^{-2}$  g,  $1.59 \times 10^{-4}$  mol) were placed into a round-bottom wide-neck glass reactor (250 mL capacity). The reactor was closed with a three-neck flat flange lid equipped with a mechanical stirrer and a torque meter which gives an indication of the viscosity of the reaction melt. The reactor was immersed into a salt bath preheated at 210°C. A heating band set at 85°C was applied around the lid. The first stage was conducted at atmospheric pressure under nitrogen flow and the mixture was allowed to react for 60 min under stirring (400 rpm) with continuous removal of methanol. The second stage was started by gradually decreasing the pressure to 0.11 mbar while the temperature was raised to the final value of 250°C. These conditions were reached within 60 min, using a linear gradient of temperature and pressure, and maintained for 3 h. Temperature of the heating band was 95°C. A light yellow product was discharged from the reactor.

**Phosphonium Salts Synthesis.** The ionic liquids used, as described in Table I, are not commercially available and their synthesis followed the protocol reported by Livi *et al.*<sup>12,13</sup> Reactions carried out are shown in Scheme 1 (octadecyltriphenylphosphonium iodide and bromide salts) and Scheme 2 (octadecyltriphenylphosphonium with tetrafluoroborate anion).

**Table I.** Thermal Degradation of the Ionic Liquids

Sample	$T_{onset}^a$ (°C)	$T^{10}_D^b$ (°C)
C <sub>18</sub> -PPH <sub>3</sub> <sup>+</sup> Br <sup>-</sup>	322	312
C <sub>18</sub> -PPH <sub>3</sub> <sup>+</sup> I <sup>-</sup>	323	318
C <sub>18</sub> -PPH <sub>3</sub> <sup>+</sup> BF <sub>4</sub> <sup>-</sup>	356	351

<sup>a</sup> Measured by TGA under N<sub>2</sub> flow at 20°C·min<sup>-1</sup>.

<sup>b</sup> 10% of weight loss temperatures measured by TGA under N<sub>2</sub> flow at 20°C·min<sup>-1</sup>.

**Synthesis of Octadecyltriphenylphosphonium Iodide ( $C_{18}\text{-PPH}_3^+\text{I}^-$ ).** Triphenylphosphine (6.12 g,  $2.33 \times 10^{-2}$  mol, 1 eq) and octadecyl iodide (8.89 g,  $2.33 \times 10^{-2}$  mol, 1 eq) were placed in a 100 mL three necked bottom flask under a positive nitrogen pressure. The stirred suspension was allowed to react for 24 h at 120°C in toluene (40 mL) under reflux to avoid evaporation of the solvent. Subsequently, the dark brown solution was left in a cold store into an ice bath, until a yellow precipitate formed. The reaction mixture was then filtered and repeatedly washed with hexane (250 mL). Most of the solvent was removed under vacuum and the product was dried to a constant weight to give a white solid (13.9 g). The structure of the salt was confirmed by  $^1\text{H}$  NMR spectroscopy.  $^1\text{H}$  NMR (400 MHz,  $\text{CDCl}_3$ ,  $\delta$ ): 7.8 (m, 15H, Ar H), 3.7 (bs, 2H;  $\text{CH}_2\text{-P}^+$ ), 1.6 (bs, 2H;  $\text{CH}_2$ ), 1.2 (m, 30H;  $\text{CH}_2$ ), 0.9 (t, 3H;  $\text{CH}_3$ ).

**Synthesis of Octadecyltriphenylphosphonium Bromide ( $C_{18}\text{-PPH}_3^+\text{Br}^-$ ).** Triphenylphosphine (10.0 g,  $3.80 \times 10^{-2}$  mol, 1 eq) and octadecyl bromide (12.7 g,  $3.80 \times 10^{-2}$  mol, 1 eq) were placed in a 250 mL three necked bottom flask, under nitrogen atmosphere. The stirred suspension was allowed to react for 24 h at 120°C in toluene (40 mL) and a white viscous liquid was formed. After cooling at room temperature, a white solid was obtained. The reaction mixture was then filtered and repeatedly washed with hexane. The structure of the salt was confirmed by  $^1\text{H}$ -NMR spectroscopy.

**Synthesis of Octadecyltriphenylphosphonium Tetrafluoroborate ( $C_{18}\text{-PPH}_3^+\text{BF}_4^-$ ).** Octadecyltriphenylphosphonium iodide (10.0 g,  $1.63 \times 10^{-2}$  mol, 1 eq) was dissolved into dichloromethane (50 mL) in a 100 mL flask. The mixture was stirred for 30 min at room temperature. At the same time, 10 mL (14.8 g,  $8.18 \times 10^{-2}$  mol, 5 eq) of a 48 wt % water solution of hydrogen tetrafluoroborate ( $\text{HBF}_4$ ), were withdrawn, diluted with 40 mL of water and stirred for 30 min at room temperature.

The two solutions were then combined and allowed to react for 24 h at room temperature under magnetic stirring. The reaction mixture was then introduced in a separatory funnel and the organic layer was repeatedly washed with distilled water (6  $\times$  50 mL). The mixture was dried over anhydrous magnesium sulphate and filtered. The solvent was removed by evaporation under vacuum and the product was dried to a constant weight to give a white solid (9.00 g). The structure of the salt was confirmed by  $^1\text{H}$  NMR spectroscopy.

**Organic Modification of Montmorillonite.** The intercalation of the organic salts into the  $\text{MMT-Na}^+$  galleries was carried out by a cationic exchange reaction. Dellite HPS (8.00 g,  $1.02 \times 10^{-2}$  mol, 1 eq) was dispersed into 160 mL of water at 60°C under vigorous stirring for 1 h. Then, the suspension was heated at 75°C and a solution of octadecyltriphenylphosphonium tetrafluoroborate (7.02 g,  $1.23 \times 10^{-2}$  mol, 1.2 eq) in 60 mL of ethanol, at 60°C, was added dropwise under vigorous stirring. The coprecipitation time was 90 min and the molar ratio clay/phosphonium salt was 1/1.2. After 3 h, the reaction mixture was cooled at room temperature and filtered, without washing. Finally, the organo-montmorillonite was dried under vacuum at 65°C for 24 h to obtain a light brown solid (13.5 g).

**Table II.** Interlayer Distance and Thermal Degradation of Unmodified and Modified Clays

Sample	Interlayer distance <sup>a</sup> (Å)	$T_{\text{onset}}$ <sup>a</sup> (°C)	$T_{10\%}^{\text{D}}$ <sup>b</sup> (°C)
MMT- $\text{Na}^+$	12.5	/	667
MMT- $\text{NR}_4^+$	18.5	206	263
MMT <sub>w</sub> - $\text{PR}_4^+\text{Br}^-$	(30.2)–22.3	319	343
MMT- $\text{PR}_4^+\text{BF}_4^-$	(30.0)–21.4	320	342
MMT <sub>w</sub> - $\text{PR}_4^+\text{BF}_4^-$	34.0	352	376

<sup>a</sup> Determined by the first reflection by XRD analysis.

<sup>b</sup> 10% of weight loss temperatures measured by TGA under  $\text{N}_2$  flow at 20°C·min<sup>-1</sup>.

In the case of octadecyltriphenylphosphonium bromide the procedure was just about the same but the product after filtration was washed several times with deionised water until complete elimination of bromide anions, checked by silver nitrate test. It was then washed with ethanol. Finally, the organo-montmorillonite was dried under vacuum at 65°C for 24 h to obtain a light brown solid.

The samples, as summarized in Table II, are denoted as  $\text{MMT-x}^+\text{y}^-$ , where  $\text{x}^+$  is the cation and  $\text{y}^-$  is the counteranion, both derived from the organic modification. The subscript “w”, if present, indicates that the sample is subjected to washing. The sample  $\text{MMT}_w\text{-PR}_4^+\text{BF}_4^-$  was washed according the described procedure.

**Preparation of Nanocomposites by *In Situ* Polymerization.** The nanocomposites were prepared in a two-stage process, from dimethyl adipate, 1,4-cyclohexanedimethanol and the organo-modified montmorillonites (3 wt % of the final product).

DMA (25.0 g,  $1.44 \times 10^{-1}$  mol) and  $\text{MMT-x}^+\text{y}^-$  (1.09 g) were placed into a round-bottomed wide-neck glass reactor (250 mL capacity). The reactor was closed with a three-neck flat flange lid equipped with a mechanical stirrer and a torque meter. The mixture was stirred vigorously (396 rpm) at room temperature for 30 min under nitrogen atmosphere.  $\text{CHDM}_{66}$  (24.8 g,  $1.72 \times 10^{-1}$  mol) and TBT ( $5.40 \times 10^{-2}$  g,  $1.59 \times 10^{-4}$  mol) were then added and the reactor was immersed into a salt bath preheated at 190°C for 60 min under stirring (298 rpm) with continuous removal of methanol. Afterwards, a heating band set at 85°C was applied around the lid and the temperature of the reaction mixture was increased to 210°C and allowed to react for 120 min.

The second stage was started by gradually decreasing the pressure to 0.06 mbar while the temperature was raised to the final value of 250°C under stirring (219 rpm). These conditions were reached within 60 min, using a linear gradient of temperature and pressure and maintained for 2 h 35 min. The temperature of the heating band was 95°C. The product discharged from the reactor was transparent in melt and light brown.

The composites are called  $\text{PCHA-MMT-x}^+\text{y}^-$ , where  $\text{MMT-x}^+\text{y}^-$  is the code of the organo-modified MMT. All the samples are listed in Table III.

**Table III.** Molecular Characteristics and Thermal Degradation of Composites

Sample	Cis/trans <sup>a</sup> (mol %)	$M_w \cdot 10^{-3b}$	$M_w/M_n^b$	$T_{onset}^c$ (°C)	$T_{10}^c$ (°C)
PCHA	35/65	94	3.7	390	371
PCHA-MMT-Na <sup>+</sup>	35/65	110	3.7	384	368
PCHA-MMT <sub>w</sub> -PR <sub>4</sub> <sup>+</sup> Br <sup>-</sup>	35/65	60	2.5	387	368
PCHA-MMT-PR <sub>4</sub> <sup>+</sup> BF <sub>4</sub> <sup>-</sup>	35/65	41	2.6	379	357
PCHA-MMT <sub>w</sub> -PR <sub>4</sub> <sup>+</sup> BF <sub>4</sub> <sup>-</sup>	35/65	24	2.8	372	345

<sup>a</sup>Ratio cis/trans of the 1,4-cyclohexylene ring in polymers, calculated from <sup>1</sup>H NMR.

<sup>b</sup> $M_w$  is the weight average molecular weight,  $M_w/M_n$  the molecular weight distribution, measured by GPC in CHCl<sub>3</sub>.

<sup>c</sup>10% of weight loss temperatures measured by TGA under N<sub>2</sub> flow at 10°C·min<sup>-1</sup>.

### Measurements

Salts and clays were characterized by ATR Fourier Transform Infrared Spectroscopy using a Perkin-Elmer Spectrum One FTIR Spectrometer equipped with a Universal ATR Sampling Accessory.

The X-ray diffraction measurements (XRD), in steps of 0.07°, over  $2\theta$  range of 1.97–60° for clay samples and over  $2\theta$  range of 2.1–35° for composites, were carried out at room temperature with two Bragg/Brentano diffractometers (Philips PW1710 for clays and XPERT-PRO for composites) with Cu K $\alpha$  radiation ( $\lambda = 0.154$  nm, monochromatization by primary graphite crystal) generated at 40 mA and 40 kV. A flat sample holder, 1.5 mm deep, was filled with sample powder.

The <sup>1</sup>H NMR spectra were recorded at room temperature on samples dissolved in CDCl<sub>3</sub> using a Varian Mercury 400 spectrometer, the frequency being 400 MHz (chemical shift are in part per million down-field from TMS).

The thermogravimetric analysis (TGA) was performed using a TGA4000 thermobalance under nitrogen atmosphere (gas flow 40 mL·min<sup>-1</sup>) from 50°C to 800°C, with a heating rate of 20°C·min<sup>-1</sup> for clays and 10°C·min<sup>-1</sup> for the homopolymer and nanocomposites. The onset degradation temperatures ( $T_{onset}$ ) were taken from the intersections of the tangents of the initial points and the inflection points; the 10% mass loss temperatures ( $T_{10}^D$ ) were measured and reported in Tables I–III.

The calorimetric analysis was carried out by means of a Perkin-Elmer DSC6, equipped with an intracooler. The measurements were performed under nitrogen flow. In order to cancel the previous thermal history, the samples (ca. 10 mg) were initially heated at 20°C·min<sup>-1</sup> to 200°C, kept at high temperature for 1 min and then cooled to -60°C at 10°C·min<sup>-1</sup>. They were kept at low temperature for 5 min. After this thermal treatment, the samples were analyzed by heating from -60°C to 200°C at 10°C·min<sup>-1</sup> (2<sup>nd</sup> scan). During the cooling scan the crystallization temperature ( $T_c$ ) and the enthalpy of crystallization ( $\Delta H_c$ ) were measured. During the 2<sup>nd</sup> scan the glass transition temperature ( $T_g$ ), melting temperature ( $T_m$ ), and enthalpy of fusion ( $\Delta H_m$ ) were measured.  $T_g$  was taken as the midpoint of the heat capacity increment associated with the glass-to-rubber transition.

Specimens for dynamic mechanical measurements were obtained by injection molding in a MiniMix Molder (Custom Scientific Instruments) equipped with a rectangular mold (30 ×

8 × 1.6 mm<sup>3</sup>). The molded samples were rapidly cooled in water and then dried in a desiccator overnight.

Dynamic mechanical measurements were performed with a dynamic mechanical thermal analyzer (Rheometrics Scientific, DMTA IV), operated in the dual cantilever bending mode, at a frequency of 3 Hz and a heating rate of 3°C·min<sup>-1</sup>, over a temperature range from -50°C to a final temperature of 100°C.

## RESULTS AND DISCUSSION

### Clay Modification

In this study new composites, based on PCHA (Figure 1) and Dellite, have been prepared by *in situ* polymerization. Two kinds of clays were used (Table II): a commercial Dellite HPS, which is not modified, and different samples of organically modified Dellite. Firstly, a commercial sample, Dellite 43b, containing ammonium salt, was tested. Moreover, Dellite HPS was modified with octadecyltriphenylphosphonium bromide and octadecyl triphenylphosphonium tetrafluoroborate. The syntheses of the phosphonium salts were carried out following Livi's protocol,<sup>12,13</sup> according to Schemes 1 and 2. In the case of tetrafluoroborate anion a large excess of reactant was used (1 : 5 vs 1 : 2 of ref. cited) in order to facilitate the exchange process between I<sup>-</sup> and BF<sub>4</sub><sup>-</sup> anions. Two samples, washed and unwashed were prepared with octadecyl triphenylphosphonium tetrafluoroborate, while only one washed sample was prepared with octadecyltriphenylphosphonium bromide. Indeed, when bromide is used as counteranion, it is necessary to eliminate it from the surface of clay, while the same is not required with tetrafluoroborate.

Figure 2 shows the thermogravimetric curves of the phosphonium salts and Table I reports the corresponding data. It is worth noting that C<sub>18</sub>-PPh<sub>3</sub><sup>+</sup>Br<sup>-</sup> and C<sub>18</sub>-PPh<sub>3</sub><sup>+</sup>I<sup>-</sup> lose weight in a single step; the maximum degradation temperature is 348°C for bromide and 359°C for iodide anion, while  $T_{onset}$  in both cases is around 322°C. The use of fluorinated anion, whose salt shows two weight losses with maximum peak at 385°C and 450°C, provides an increase in the thermal stability of the ionic liquid, not new in literature.<sup>12</sup> The onset degradation temperature is 356°C (Table I). Such a behavior can be justified by considering that the phosphonium salts are generally capable of undergoing a wide range of reactions because of the greater steric tolerance of the phosphorus atom and the participation of its low-lying d-orbitals in the processes of making and breaking chemical bonds during degradation.<sup>4</sup>

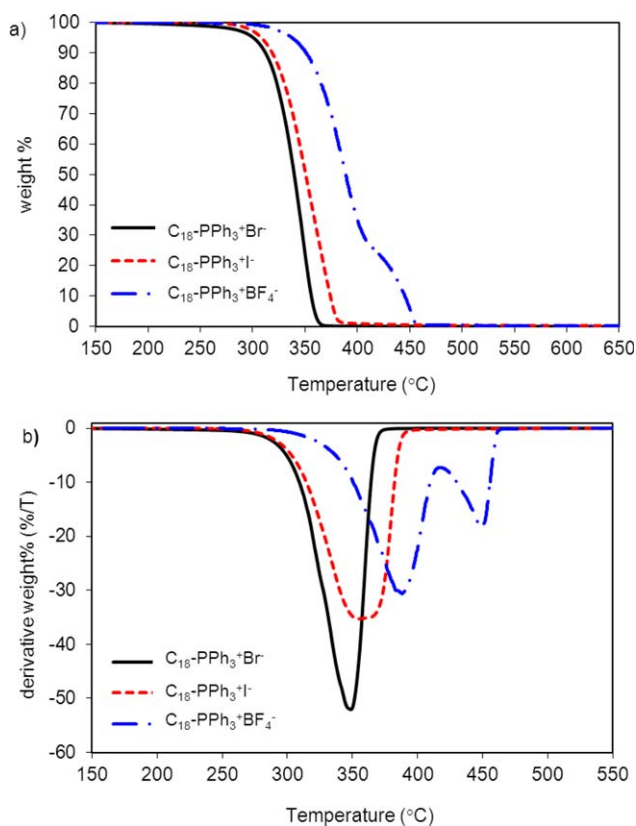


**Figure 2.** (a) TGA thermograms of octadecyltriphenylphosphonium salts and (b) corresponding derivative weight %. [Color figure can be viewed in the online issue, which is available at [wileyonlinelibrary.com](http://wileyonlinelibrary.com).]

The XRD patterns for pristine clay (MMT- $\text{Na}^+$ ) and the organoclays are shown in Figure 3, while the crystallographic data are summarized in Table II. The interlayer distance can be extrapolated from the first reflection peak  $d_{001}$ , positioned at  $2\theta = 7.0^\circ$ , corresponding to 12.5 Å in case of the precursor clay and according to literature.<sup>14,15</sup> As expected, the organic modification of the clay resulted in an increase in the basal spacing, causing a large shift in the diffraction peak towards lower values of  $2\theta$ , explained by the swelling of layered silicates because of the steric volume occupied by the three ring functions and the alkyl chain.

The montmorillonites modified with the phosphonium salts show similar profiles. Three reflections are present in both curves into the region  $2\theta = (2-10)^\circ$ . More in detail, they are located at  $2\theta = 4.1^\circ$  ( $d = 21.4$  Å),  $6.1^\circ$  ( $d = 14.5$  Å) and  $8.2^\circ$  ( $d = 10.8$  Å) in MMT- $\text{PR}_4^+\text{BF}_4^-$  and  $2\theta = 3.9^\circ$  ( $d = 22.3$  Å),  $6.1^\circ$  ( $d = 14.5$  Å), and  $8.0^\circ$  ( $d = 11.0$  Å) in MMT- $\text{w-PR}_4^+\text{Br}^-$ . The first reflection, corresponds to the basal peak (001) and it is associated to the third reflection, which correlates the (002) plane of the organoclay layers. Nevertheless the second reflection suggests the possible presence of a second basal peak at  $2\theta = 2.6^\circ$ , resulting in a  $d$ -spacing of almost 30 Å, as confirmed by a WAXD analysis conducted at lower angle by changing the slits of the instrument [Figure 3(c)]. The presence of two basal peaks suggests that two different orientations, conferring two layers distances, are present. In literature, the  $d$ -spacing for the

same organoclays is reported to be 19.5 Å,<sup>16</sup> or 42 Å,<sup>13</sup> thus probably a paraffin type monolayer orientation is present.<sup>17,18</sup> The other commercial MMT tested for comparison was Dellite 43b, containing dimethyl benzyl hydrogenated tallow ammonium ion; it resulted to have an interlamellar space higher than Dellite HPS:  $d_{001}$  was 18.5 Å ( $2\theta = 4.7^\circ$ ), according to literature.<sup>19</sup>

In Figure 4 the ATR-FTIR profiles of pristine and organo-modified MMTs are shown: the slight band near  $3600\text{ cm}^{-1}$  is because of  $-\text{OH}$  stretching mode of  $\text{Al-OH}$  and  $\text{Si-OH}$  of MMT; a weak intensity band at  $1630\text{ cm}^{-1}$  is because of  $-\text{OH}$  bending vibration of adsorbed water, while at 1100 and  $1000\text{ cm}^{-1}$  the Si-O stretching out-of-plane and in-plane vibrations of layered silicate are present. At low wavenumber

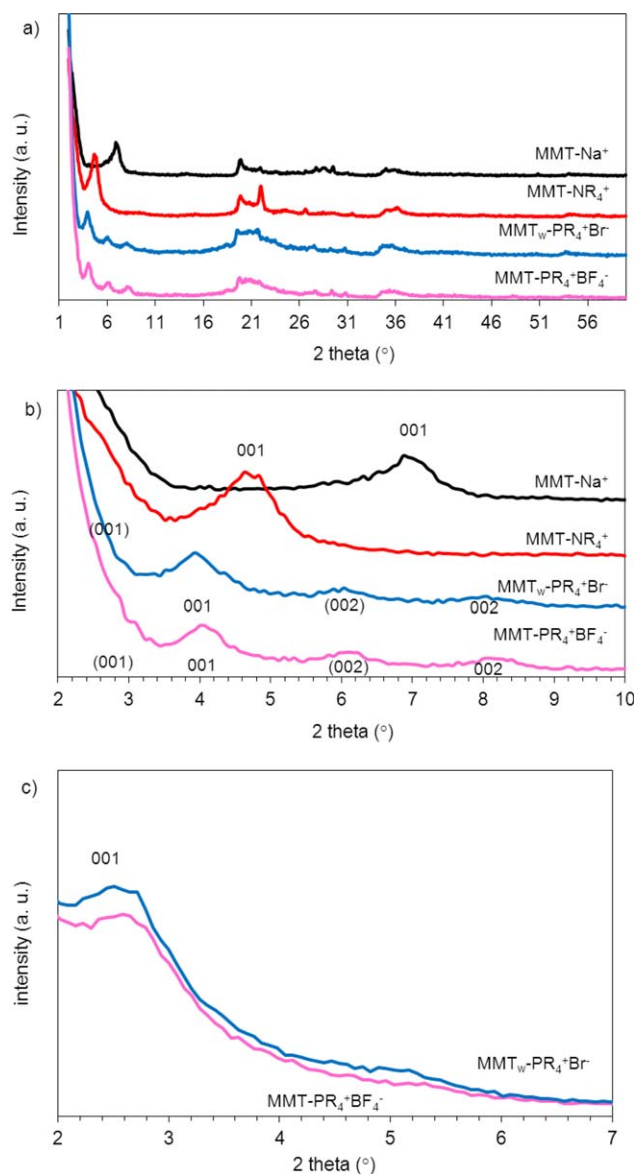


**Figure 3.** (a) XRD profiles of modified and unmodified clays; (b) zoom region in the range  $2\theta = 2-10^\circ$ ; and (c) XRD analysis of MMT- $\text{PR}_4^+\text{BF}_4^-$  and MMT- $\text{w-PR}_4^+\text{Br}^-$  conducted at low angle. [Color figure can be viewed in the online issue, which is available at [wileyonlinelibrary.com](http://wileyonlinelibrary.com).]

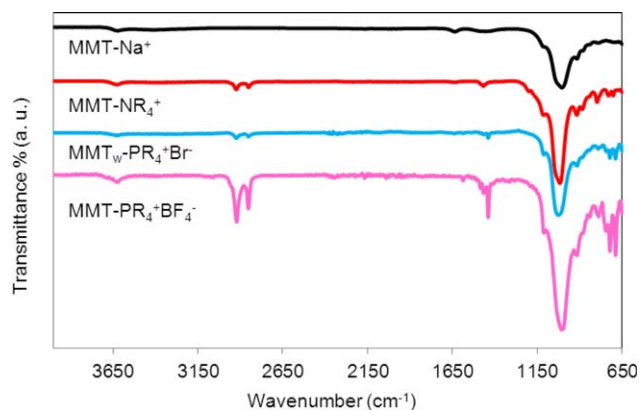


**Figure 4.** FTIR curves of modified and unmodified clays. [Color figure can be viewed in the online issue, which is available at [wileyonlinelibrary.com](http://wileyonlinelibrary.com).]

(900–830  $\text{cm}^{-1}$ ) Al-Al-OH, Al-Fe-OH, Al-Mg-OH bending vibrations are found. The asymmetric and symmetric vibration of methylene groups ( $-\text{CH}_2$ ) of the aliphatic chain appear (2900  $\text{cm}^{-1}$ ) in ammonium and phosphonium-modified clays; in addition the phenyl- $\text{P}^+$  vibration is clearly present at 1438  $\text{cm}^{-1}$ , as well as the double C=C bond in phenyl groups (1600–1400  $\text{cm}^{-1}$ ), proving that the phosphonium modification of montmorillonite is successfully carried out.<sup>15,20</sup>

In Figure 5 and in Table II the thermogravimetric curves and data of the original and modified MMTs are reported. The degradation of the modified clays occurs in two steps. The first step indicates the presence of organics simply physisorbed. Indeed, as a general rule, evolution of absorbed water and gas species, such as physisorbed  $\text{CO}_2$  and  $\text{N}_2$ , occurs below 180°C. The second step corresponds to organics intercalated into clay galleries,<sup>13</sup> as organic substances evolve from 250°C to 500°C. Dehydroxylation of the aluminosilicate occurs from 500°C to 700°C and evolution of products associated with residual organic carbonaceous residue occurs between 700°C and 1000°C. The curves clearly indicate that the most thermally stable is  $\text{MMT-Na}^+$  because of the absence of an organic modifier, while the less stable is  $\text{MMT-NR}_4^+$ , in agreement with literature data.<sup>1</sup>

Moreover, it must be underlined that the presence of the ammonium salt causes a strong decrement in the thermal stability of the pristine MMT. Actually, the sample begins to lose weight at about 206°C. Therefore, this material cannot be used during *in situ* polymerization of PCHA, that is performed in the 210–250°C temperature range.

On the other hand, the enhanced thermal stability of the  $\text{C}_{18}\text{-PR}_4^+\text{Br}^-$  and  $\text{C}_{18}\text{-PR}_4^+\text{BF}_4^-$  salts is evident in the modified clays. The  $T_{\text{onset}}$  is the same in  $\text{MMT-w-PR}_4^+\text{Br}^-$  and  $\text{MMT-PR}_4^+\text{BF}_4^-$  ( $\approx 319^\circ\text{C}$ ), showing no difference between the counterions. In general the literature reports that tetrafluoroborate anion has a higher stabilizing effect with respect to the bromide anion.<sup>12,21</sup> The observed behavior could be explained in terms of the presence of physisorbed organic salt, which determines a faster degradation: the  $\text{MMT-PR}_4^+\text{BF}_4^-$  sample, in fact, is not

subjected to washing. It is important to highlight that, when bromide is used as counteranion, it is necessary to thoroughly eliminate it by long washing, while the same is not required with tetrafluoroborate. Indeed, the physically adsorbed phosphonium salts on the layer edges have a key role in the preparation of nanocomposites as they act as compatibilizing agents and allow to reach a very fine dispersion state and better mechanical performances.<sup>13</sup>

In order to check the effect of washing and therefore the presence of physisorbed  $\text{BF}_4^-$  counter anion on the clay thermal stability and on the final polymer composites, a part of  $\text{MMT-PR}_4^+\text{BF}_4^-$  was washed and analyzed (sample denoted  $\text{MMT-w-PR}_4^+\text{BF}_4^-$  in Table II). As expected the sample turned out to be the most thermally stable among the organo-modified clays, with a  $T_{\text{D}}^{10} = 376^\circ\text{C}$  (with a  $\Delta T^{10} = +33^\circ\text{C}$  as compared to the other modified clays), thus confirming the above-mentioned statements.

Finally, all the residues of the thermograms in Figure 5 are coherent with the inorganic content. In fact,  $\text{MMT-Na}^+$  has the highest residue (87 wt %), the clays exchanged with organic cations and subjected to washing have a residue of around 60 wt %, while the one not washed,  $\text{MMT-PR}_4^+\text{BF}_4^-$ , has the lowest residue (43 wt %).

#### Preparation of Nanocomposites by *In Situ* Polymerization

The composites, with a 3 wt % of pristine MMT and organo-modified montmorillonites, were prepared by *in situ* polymerization according to the procedure described in ref. 14. Such procedure includes a pre-stage, in which diol and modified clay are charged into the reactor to favor the swelling of the MMT. After this pre-stage the catalyst and DMA are added, then a typical two-stage polycondensation process is applied. The montmorillonite modified with ammonium salt was not used, as it is not thermally stable in polymerization conditions.

The final materials were analyzed by  $^1\text{H-NMR}$  analysis which confirmed the success of the polymerization and the molecular structure reported in Figure 1 (data not shown). Moreover, by focusing on the two distinct peaks located at around 4.0 ppm

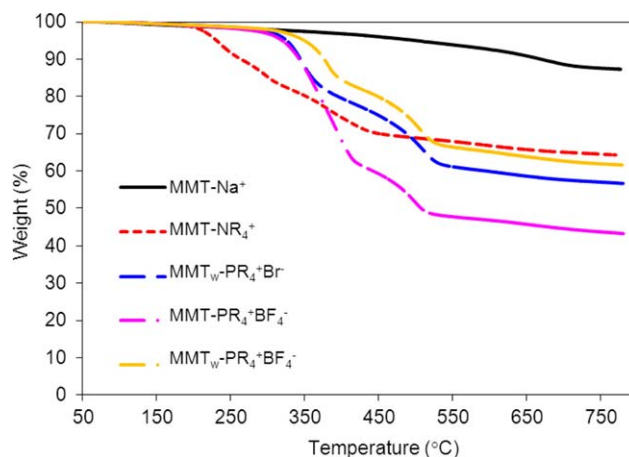


**Figure 5.** TGA thermograms of modified and unmodified clays. [Color figure can be viewed in the online issue, which is available at [wileyonlinelibrary.com](http://wileyonlinelibrary.com).]

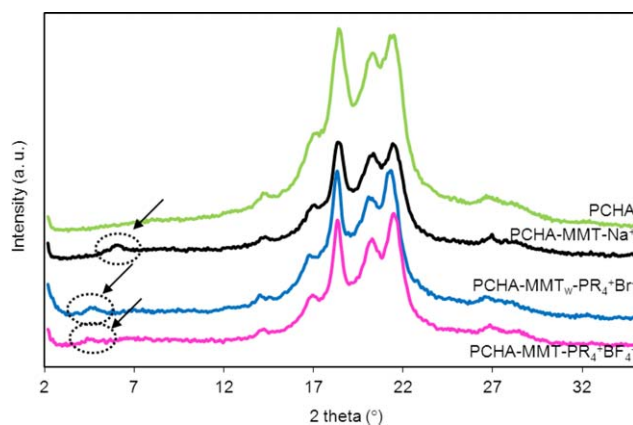


**Figure 6.** XRD profiles of homopolymer and PCHA-MMT- $x^+y^-$  composites. [Color figure can be viewed in the online issue, which is available at [wileyonlinelibrary.com](http://wileyonlinelibrary.com).]

and related to the protons in cis and trans configurations, it was observed that isomerization processes from trans to cis forms do not take place during polymerization.

All the composites were characterized by GPC analysis and the molecular weight values, reported in Table III, are high, except in case of PCHA-MMT<sub>w</sub>-PR<sub>4</sub><sup>+</sup>BF<sub>4</sub><sup>-</sup> ( $M_w = 24,000$ ). For this reason the sample has been characterized but it has not been compared to the other composites.

The degree of dispersion of the organo-modified clay in PCHA matrix was evaluated by XRD analysis. In Figure 6 XRD profiles of PCHA-MMT- $x^+y^-$  nanocomposites were compared: reflections related to the polymer are present in the  $2\theta = 15\text{--}25^\circ$  region. As highlighted in the said Figure, all the composites feature the diffraction line of the starting modified clay, suggesting that the structures are partially intercalated. In addition, from XRD profile of neat PCHA a crystallinity degree of 52.9% ( $\pm 1.1$ ) was calculated.

Figure 7 reports the TGA thermograms of the composites, while the thermal data are shown in Table III. First of all, as can be

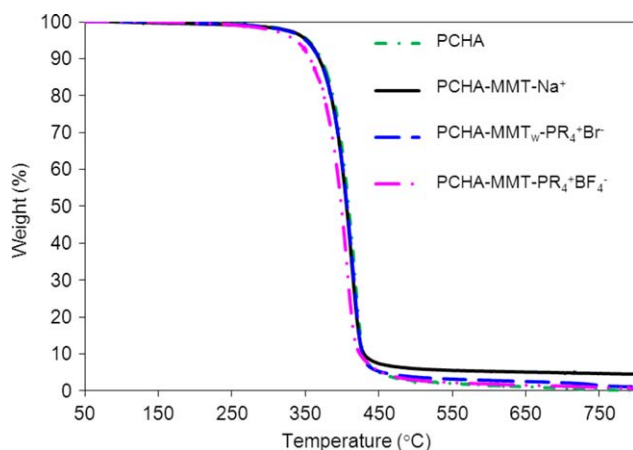


**Figure 7.** TGA thermograms of homopolymer and PCHA-MMT- $x^+y^-$  composites. [Color figure can be viewed in the online issue, which is available at [wileyonlinelibrary.com](http://wileyonlinelibrary.com).]

**Table IV.** Thermal Properties of Composites

Sample	$T_g^a$ (°C)	$T_C^b$ (°C)	$\Delta H_C^b$ (J.g <sup>-1</sup> )	$T_m^a$ (°C)	$\Delta H_m^a$ (J.g <sup>-1</sup> )
PCHA	-20	61	37	108	30
PCHA-MMT-Na <sup>+</sup>	-22	44	33	104	29
PCHA-MMT <sub>w</sub> -PR <sub>4</sub> <sup>+</sup> Br <sup>-</sup>	-19	49	35	106	32
PCHA-MMT-PR <sub>4</sub> <sup>+</sup> BF <sub>4</sub> <sup>-</sup>	-19	45	32	105	32
PCHA-MMT <sub>w</sub> -PR <sub>4</sub> <sup>+</sup> BF <sub>4</sub> <sup>-</sup>	-23	54	39	100	36

<sup>a</sup> Measured by DSC during the 2<sup>nd</sup> heating scan at 10°C.min<sup>-1</sup>.

<sup>b</sup> Measured by DSC during the cooling scan at 10°C.min<sup>-1</sup>.

seen, samples lose weight in one main decomposition process, in the 300–450°C range. The data in Table III indicate that the most stable sample is the homopolymer, followed by the PCHA-MMT-Na<sup>+</sup> sample. Then, a slightly negative effect of the organo-clays on the thermal stability of the polymeric matrix can be observed. The accelerating decomposition effect is mainly because of: (i) the presence of hydroxyl groups on the edges of the clay, that could catalyse polymer decomposition; (ii) the existence of active catalytic sites, that affects the polymer degradation; and (iii) the degradation of the clay, that forms a protonated silicate, which in turn catalyses the degradation of the polymer.

In general the literature reports discordant results on the subject. Some papers report the enhanced thermal stability of nanocomposites containing phosphonium-modified clays,<sup>14,22,23</sup> even though in some cases the enhancement is not remarkable.<sup>13</sup>

Xiao *et al.*<sup>24</sup> recently discussed the catalysing degradation effect of a modified MMT on polycarbonate chains, resulting in a decrease in thermal stability. On the other hand Chang *et al.*,<sup>25</sup> in their studies of intercalated nanocomposites with poly(butylene terephthalate) (PBT) incorporated between the montmorillonite layers, found more thermal stability for hybrids than pure PBT.

Chrissafis *et al.*<sup>26</sup> clarify this contradictory effect. They clearly reported that in case of composites with organo-modified clay,

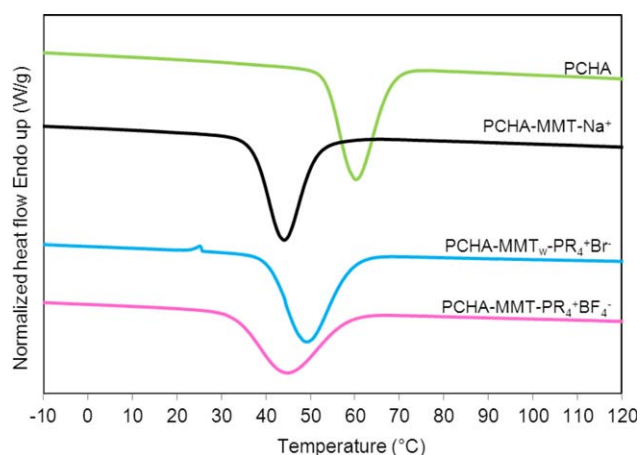


**Figure 8.**  $T_C$  profiles obtained by DSC during the cooling scan for homopolymer and PCHA-MMT- $x^+y^-$  composites. [Color figure can be viewed in the online issue, which is available at [wileyonlinelibrary.com](http://wileyonlinelibrary.com).]

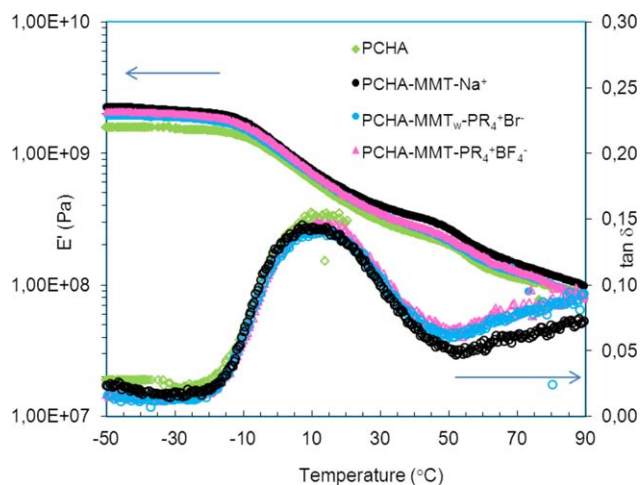


**Figure 9.** DMTA spectra for homopolymer and PCHA-MMT- $x^+y^-$  composites. Storage Modulus ( $E$ ) and  $\tan \delta$  as a function of temperature. [Color figure can be viewed in the online issue, which is available at [www.wileyonlinelibrary.com](http://www.wileyonlinelibrary.com).]

the achieved clay dispersion (intercalated-exfoliated) as well as the used modifier can alter the thermal decomposition of polymers; cationic compounds used for organo-modification of MMT have a negative effect on thermal degradation while the exfoliated structure because of the finer dispersion of the clay nanoparticles can lead to thermal stabilization than the intercalated structure.

In any case, the degradation temperatures of the composites are consistently higher as compared to the polymerization temperature process, therefore it could be argued that degradation phenomena are not present during the polymerization process.

The thermal properties of PCHA hybrids are listed in Table IV. The glass transition temperatures ( $T_g$ ) of the composites remained fairly constant with respect to the homopolymer ( $\approx -20^\circ\text{C}$ ). The inclusion of clay into the polymer matrix is reported to increase  $T_g$ , as a result of the confinement of the polymer chains into the intra-gallery of the layered structure in the intercalated polymer/clay nanocomposite.<sup>27,28</sup> The inability of the clay platelets to restrict the bond segmental motion of the polymer chains, resulting in an unaffected  $T_g$ , could suggest a good dispersion of the clays into the matrix despite the results of the XRD analysis.<sup>22</sup> The melting peak of the pure PCHA appears at  $108^\circ\text{C}$ : a slight decrease is present in the sample with pristine MMT- $\text{Na}^+$  ( $104^\circ\text{C}$ ), and in those with the phosphonium salts ( $\approx 105^\circ\text{C}$ ).

A more marked difference is evident considering the crystallization temperature ( $T_c$ ): all composites crystallize at lower temperatures compared to the homopolymer (Figure 8). It is worth noting that the PCHA-MMT- $\text{PR}_4^+\text{BF}_4^-$  composite shows a wide exothermal peak. This could suggest a slower crystallization process. Such behavior might stem from the fact that the movements of the polymer chains in the melt are restricted by the clay platelets which act as obstacles for the mobility of the chains to join the crystallization growth front. This behavior

suggests an homogeneous dispersion of the clays in the PCHA matrix.<sup>3</sup>

The dynamic mechanical properties of PCHA-MMT samples were also investigated. Figure 9 shows the dynamic storage modulus ( $E'$ ) as a function of temperature. As can be seen, the values of  $E'$  for composites are slightly higher than that of PCHA homopolymer, across the whole temperature range. This moderate enhancement in storage modulus may be associated with a reinforcing effect imparted by the high aspect ratio of clay platelets, causing a greater degree of stress transfer at the interface.<sup>29</sup> Moreover the restricted segmental motion of the PCHA chains at the organic/inorganic interface, originating from the good degree of distribution of clay platelets, might also be responsible for the enhancement in storage modulus.<sup>22</sup>

Furthermore, considering the  $\tan \delta$  (variation of the damping factor) maximum peak visible in Figure 9, the homopolymer and the composites with the organo-modified MMT display a  $T_g$  of  $10^\circ\text{C}$ . This result is in agreement with the DSC data, underlying that the presence of nanoclay does not affect  $T_g$ .

## CONCLUSIONS

In this study novel composites, containing clays organo-modified with ionic liquids based on phosphonium salts, were prepared by direct polymerization from monomers. This procedure is possible thanks to the high thermal stability of the salts. The clays result to have a good degree of dispersion in the polymeric matrix, despite the intercalated structure of composites. The composites present moderately enhanced mechanical properties and are characterized by the same thermal stability of the matrix. Finally, the materials based on PCHA also have the advantages to be potentially biobased and biodegradable.

Therefore, it has been proven that it is possible to obtain new composites by *in situ* polymerization using clays modified with phosphonium salts. The high thermal stability of these materials can be very useful for all the applications where high processing temperatures are necessary. A new class of high-performance materials can thus be easily obtained.

## REFERENCES

- Leszczyńska, A.; Njuguna, J.; Pielichowski, K.; Banerjee, J. R. *Thermochim. Acta* **2007**, *453*, 75.
- Awad, W. H.; Gilman, J. W.; Nyden, M.; Harris, R. H. Jr.; Sutto, T. E.; Callahan, J.; Trulove, P. C.; DeLong, H. C.; Fox, D. M. *Thermochim. Acta* **2004**, *409*, 3.
- Sisti, L.; Totaro, G.; Fiorini, M.; Celli, A.; Coelho, C.; Hennous, M.; Verney, V.; Leroux, F. *J. Appl. Polym. Sci.* **2013**, *130*, 1931.
- Xie, W.; Xie, R.; Pan, W. P.; Hunter, D.; Koene, B.; Tan, L. S.; Vaia, R. *Chem. Mater.* **2002**, *14*, 4837.
- Celli, A.; Marchese, P.; Sisti, L.; Dumand, D.; Sullalti, S.; Totaro, G. *Polym. Int.* **2013**, *62*, 1210.
- Berti, C.; Celli, A.; Marchese, P.; Barbiroli, G.; Di Credico, F.; Verney, V.; Commereuc, S. *Eur. Polym. J.* **2009**, *45*, 2402.



7. Berti, C.; Binassi, E.; Colonna, M.; Fiorini, M.; Kannan, G.; Karanam, S.; Mazzacurati, M.; Odeh, I.; Vannini, M. U.S. Pat. **2010**, US 20100168373.
8. Berti, C.; Binassi, E.; Celli, A.; Colonna, M.; Fiorini, M.; Marchese, P.; Marianucci, E.; Gazzano, M.; Di Credico, F.; Brunelle, D. J. *J. Polym. Sci. Part B: Polym. Phys.* **2008**, *46*, 619.
9. Berti, C.; Celli, A.; Marchese, P.; Marianucci, E.; Barbiroli, G.; Di Credico, F. *Macromol. Chem. Phys.* **2008**, *209*, 1333.
10. Celli, A.; Marchese, P.; Sullalti, S.; Berti, C.; Barbiroli, G. *Macromol. Chem. Phys.* **2011**, *212*, 1524.
11. Celli, A.; Marchese, P.; Sullalti, S.; Berti, C. Eco-friendly (co)polyesters containing 1,4-cyclohexylene units: correlations between stereochemistry and phase behavior. In: *Polymer Phase Behaviour*; Ehlers, T. P.; Wilhelm, J. K., Eds.; Nova Science Publishers: New York, **2011**, pp. 205–234.
12. Livi, S.; Duchet-Rumeau, J.; Pham, T. N.; Gérard, J. F. *J. Colloid Interface Sci.* **2011**, *354*, 555.
13. Livi, S.; Duchet-Rumeau, J.; Pham, T. N.; Gérard, J. F. *J. Colloid Interface Sci.* **2010**, *349*, 424.
14. Chang, J. H.; Kim, S.; Im, S. *Polymer* **2004**, *45*, 5171.
15. Xiang, C.; Shao-zao, T.; Ma-hua, L.; Ting, W.; Ren-fu, L.; Biao, Y. *J. Cent. South Univ. Technol.* **2010**, *17*, 485.
16. Umasankar Patro, T.; Khakhar, D. V.; Misra, A. *J. Appl. Polym. Sci.* DOI 10.1002/app.
17. Liu, H. B.; Xiao, H. N. *J. Inorg. Mater.* **2012**, *27*, 780.
18. Hedley, C. B.; Yuan, G.; Theng, B. K. G. *Appl. Clay Sci.* **2007**, *35*, 180.
19. Chevillard, A.; Angellier-Coussy, H.; Peyron, S.; Gontard, N.; Gastaldi, E. *Soil Sci. Soc. Am. J.* **2012**, *76*, 420.
20. Patel, H. A.; Somani, R. S.; Bajaj, H. C.; Jasra, R. V. *Appl. Clay Sci.* **2007**, *35*, 194.
21. Byrne, C.; McNally, T. *Macromol. Rapid Commun.* **2007**, *28*, 780.
22. Suin, S.; Shrivastava, N. K.; Maiti, S.; Khatua, B. B. *Eur. Polym. J.* **2013**, *49*, 49.
23. Patro, T. U.; Khakhar, D. V.; Misra, A. *J. Appl. Polym. Sci.* **2009**, *113*, 1720.
24. Xiao, J.; Wang, S.; Lua, P.; Hub, Y. *Proc. Eng.* **2013**, *62*, 791.
25. Chang, J. H.; An, Y. U.; Kim, S. J.; Im, S. *Polymer* **2003**, *44*, 5655.
26. Chrissafis, K.; Bikiaris, D. *Thermochim. Acta* **2011**, *523*, 1.
27. Yu, Y. H.; Lin, C. Y.; Yeh, J. M.; Lin, W. H. *Polymer* **2003**, *44*, 3553.
28. Lu, H.; Nutt, S. *Macromolecules* **2003**, *36*, 4010.
29. Hasegawa, N.; Okamoto, H.; Kawasumi, M.; Usuki, A. *J. Appl. Polym. Sci.* **1999**, *74*, 3359.